Praise Worthy Prize

International Review of Electrical Engineering (I.R.E.E.), Vol. 6, N. 4
July-August 2011

The Effect of Thyristor Controlled Series Compensator on Power System Oscillation Damping Control

Ghazanfar Shahgholian, Afshin Etesami

Abstract – *The variable series compensation is highly effective in both controlling power flow in the line and in improving stability. Thyristor controlled series compensator (TCSC) is one of the most important and known series flexible ac transmission system (FACTS) controllers. This paper investigates the effects of the TCSC on small-signal power system stability. The power sensitivity model is used to the representation of the electric power system. Both IEEE type-ST1 and IEEE type-ST3 excitation system model are used. The proposed controller and technique are employed single-machine infinite-bus (SMIB) system under different cases. To validate the effectiveness of the TCSC on enhancing system stability, eigenvalues analysis and a time-domain simulation implemented on SMIB equipped with TCSC. Finally, the simulation results verify the validity of the proposed approach.*

Keywords: *FACTS Device, TCSC, Linear and Nonlinear Model, Modal Analysis, Damping Controller*

Nomenclature

σ	Condition angle
α	Thyristor angle
λ	Compensation ratio
X_T	Variable reactance of TCSC
U_T	Terminal voltage magnitude
U_B	Infinite voltage magnitude
I_T	Terminal current magnitude
K_A, T_A	Gain and time constant of AVR
E_F	Exciter output voltage
U_R	Reference voltage
δ	Angle load
ω	Angular velocity
ω_o	Base electrical angular velocity
P_M	Mechanical power input
P_E	Electrical power output
K_D	Inherent damping constant
E'_q	Voltage proportional to direct axis flux linkages
X_d, X_q	Direct and quadrature axis components of synchronous machine reactance
X'_d	Direct axis transient reactance of synchronous machine
T'_{do}	d-axis transient open-circuit time constant
i_d, i_q	Direct and quadrature axis components of armature current
u_d, u_q	Direct and quadrature axis components of terminal voltage
f_o	Operating frequency
H	Generator inertia constant

I. Introduction

Modern system development leading to increased complexity of power system topology in the study of power system. Power Systems are non-linear nature of power and dynamic linear differential equations making them equivalent to the linear system converts. The linear theory to simulate and analyze conventional system can be used. Also, various theories of structural control for linear systems in the controller design to be applied [1].

Damping improves building potential fluctuations caused by small amplitude disturbance occurred and sustainable improvement in dynamic power system control is one of the important tasks in grid power. The potential benefits of using FACTS controllers for enhancing power system stability are well known. The FACTS devices increase the transmission capacity and the active and reactive power control [2]-[4]. FACTS devices can be divided into two generations [5]. Devices in one category essentially replace mechanical switches with power electronic switches such as static var compensators (SVC), and the thyristor controlled phase shifting transformers [6], [7]. FACTS devices in the other category use the power converter, usually a voltage source converter, in combination with a dc storage element such as interline power flow controller (IPFC) and unified power flow controller (UPFC) [8]-[10].

Series connected controllers are usually employed in active power control and to improve the stability of power system. TCSC is a typical series FACTS device that is connected in series with the line conductors to compensate for the inductive reactance of the line. The series reactance is adjusted automatically, within limits, to keep

Manuscript received and revised July 2011, accepted August 2011

the specified amount of active power flow across the line. TCSC is an effective and economical means of solving problems of transient stability, dynamic stability, steady state stability and voltage stability in long transmission lines. It is much more effective than the shunt FACTS devices in the application of power flow control and power system oscillation damping control [11]. In dynamic applications of TCSC for evaluating system damping power oscillations to improve system dynamic, various control techniques and designs have been proposed in the literature [12]-[16]. The effect of TCSC on the small signal voltage stability for a simple power system with an infinitive bus, while taking into account the static load and dynamic load simultaneously discussed in [17]. A multi-objective multi-case problem of optimal allocation of three generic types of FACTS devices namely TCSC, SVC and STATCOM to be solved by an approach based on fuzzy decision making and genetic algorithm presented in [18]. A residue factor method based on the relative participation of the parameters of FACTS controller to the critical mode to find the optimal location of the three types of FACTS controllers include TCSC, SVC and UPFC is proposed in [19].

The small-signal stability problem of power system can be analyzed by eigenvalue analysis of a linearized power system about an equilibrium operation point. In this paper, the linearized model of SMIB system with and without TCSC is used to investigate the effects of the controllers on small signal power system stability. The study is based on investigation of the eigenvalue of the linearized power system model in the framework of dynamic bifurcation theory. Finally, the simulation results show the effectiveness and robustness of proposed controller to enhance system stability by damping oscillations of different disturbances.

II. Thyristor Controlled Series Compensator

A typical TCSC model as shown in Fig. 1 consists of a fixed series capacitor (FC) in parallel with a thyristor controlled reactor (TCR). The TCR is formed by a reactor in series with a bi-directional thyristor valve that is fired with a phase angle α. The combination of TCR and capacitor allow the capacitive reactance to be smoothly controlled over a wide range and switched upon command to a condition where the bi-directional thyristor pairs conduct continuously and insert an inductive reactance into the line [20]. The equivalent reactance at fundamental frequency is given by [21]:

$$X_{TCR} = X_L \frac{\pi}{\sigma - \sin\sigma} \tag{1}$$

where σ is the condition angle and X_L is the inductive reactance of the inductor L connected in parallel with C at the fundamental frequency without thyristor control.

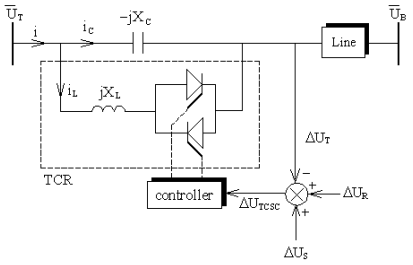

Fig. 1. A TCSC installed in a SMIB power system

The $\alpha=\pi-\sigma/2$ is the thyristor angle of valves with respect to the zero crossing instant of the controller voltage. The effect of increasing α is to increasing the effective inductance of the reactor. In effect, the TCR is a controllable susceptance. The variation in susceptance is smooth or continuous. The TCSC can be continuously controlled either in capacitive or in inductive area, avoiding the steady-state resonant region [22].

A parameter to describe the TCSC main circuit is the compensation ratio (λ), which is the quotient of the resonant frequency and the network frequency:

$$\lambda = \sqrt{\frac{X_C}{X_L}} = \frac{1}{\omega}\sqrt{\frac{1}{LC}} \tag{2}$$

where X_C is the nominal reactance of the fixed capacitor C at the fundamental frequency. Reasonable values for λ fall in the range of 2 to 4. Assuming that the total current passing through the TCSC is sinusoidal; the equivalent reactance at the fundamental frequency can be represented as a variable reactance X_T [23]-[25]:

$$X_T = X_C\left[1-\frac{\lambda^2}{\lambda^2-1}\frac{\sigma+\sin\sigma}{\pi}+ \right.$$
$$\left. +\frac{4\lambda^2\cos^2(\sigma/2)}{\pi\left(\lambda^2-1\right)^2}\left(\lambda\tan\frac{\lambda\sigma}{2}-\tan\frac{\sigma}{2}\right)\right] \tag{3}$$

Compared to the system mechanical mode, due to the fast switching characteristics of thyristors, the electrical dynamic behavior of the TCSC are very fast and can be neglected in the study of small-signal stability. The approximate model of TCSC for dynamic analysis is show in Fig. 2.

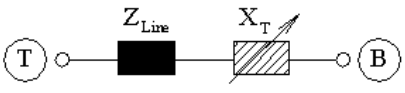

Fig. 2. TCSC mathematical model for dynamic analysis

The equivalent reactance change with the firing angles of the thyristors. The firing angle α can be controlled to take any value between 90° and 180°, corresponding to

values of σ between 180° and 0° [26]. In practice, α must be chosen in the range $90^o \le \alpha_{min} \le \alpha \le \alpha_{max} \le 180^o$. For L=3mH and C=240μF the TCSC reactance show in Fig. 3. It shows the two resonant points.

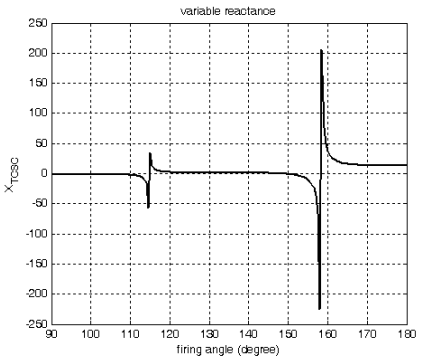

Fig. 3. Impedance characteristic curve

Fig. 4 shows the variation of the TCSC reactance against the λ and α. It can be observed that, for a given λ, the value of equivalent reactance (X_T) can be controlled by adjusting α.

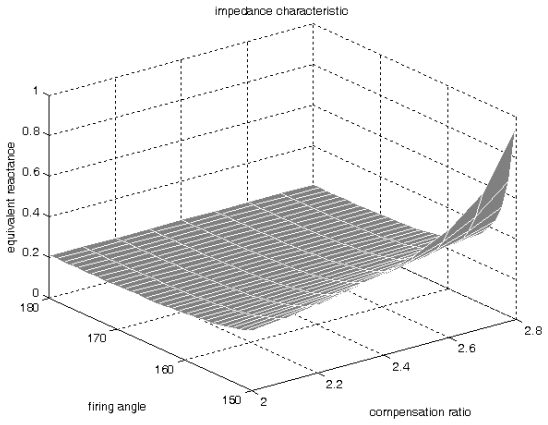

Fig. 4. Effect of firing angle and compensation ratio on equivalent reactance

III. System Description

The SMIB system with TCSC shown in Fig. 5 is considered in this study. The infinite bus is represented by a constant source voltage having a constant frequency.

The generator terminal voltage and the infinite bus voltage are represented by U_T and U_B, respectively. The generator terminal current is $i_T=i_L+i_S$, where i_S and i_L are load current and line current.

III.1. Transmission Line

The transmission line and shunt load may be represented by a two-port network, and equations can be written in terms of the ABCD constants.

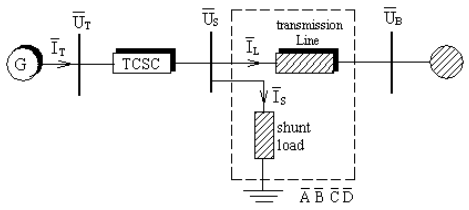

Fig. 5. Single-machine infinite-bus power system with TCSC

Referring to Fig. 5, the S bus voltage (U_S) in terms of the d and q components are:

$$\begin{cases} U_{sd} = u_d + X_T\, i_q = \underbrace{\left(X_q + X_T\right)}_{X_{qs}} i_q \\ U_{sq} = u_q - X_T\, i_d = E_q^{'} - \underbrace{\left(X_d^{'} + X_T\right)}_{X_{ds}^{'}} i_d \end{cases} \tag{4}$$

where E'_q is the machine internal voltage, i_d and i_q are the d and q components of the terminal current, X'_d and X_q are the direct and quadrature reactance of the generator. Expressing the ABCD constant in polar form as $A\angle\alpha$ and $B\angle\beta$, i_d and i_q can be written as:

$$\begin{aligned} i_d = {} & \frac{AU_{sd}}{B}\cos(\alpha-\beta) - \frac{AU_{sq}}{B}\sin(\alpha-\beta) + \\ & -\frac{U_{Bd}}{B}\cos\beta - \frac{U_{Bq}}{B}\sin\beta \end{aligned} \tag{5}$$

$$\begin{aligned} i_q = {} & \frac{AU_{sd}}{B}\sin(\alpha-\beta) + \frac{AU_{sq}}{B}\cos(\alpha-\beta) + \\ & -\frac{U_{Bq}}{B}\cos\beta + \frac{U_{Bd}}{B}\sin\beta \end{aligned} \tag{6}$$

where U_{Bd} and U_{Bq} are d and q components of the infinite bus voltage. Therefore:

$$\begin{aligned} i_d = {} & \frac{1}{\Delta}\left(\frac{AU_B X_{qs}}{B^2}\sin\alpha - \frac{U_B\cos\beta}{B}\right)\sin\delta + \\ & +\frac{1}{\Delta}\left[\frac{A^2 X_{qs}}{B^2} - \frac{A}{B}\sin(\alpha-\beta)\right]E_q^{'} + \\ & -\frac{1}{\Delta}\left(\frac{AU_B X_{qs}}{B^2}\cos\alpha + \frac{U_B\sin\beta}{B}\right)\cos\delta \end{aligned} \tag{7}$$

$$\begin{aligned} i_q = {} & \frac{1}{\Delta}\left(\frac{AU_B X_{ds}^{'}}{B^2}\cos\alpha + \frac{U_B\sin\beta}{B}\right)\sin\delta \\ & +\frac{1}{\Delta}\frac{A\cos(\alpha-\beta)}{B}E_q^{'} + \\ & +\frac{1}{\Delta}\left(\frac{AU_B X_{ds}^{'}}{B^2}\sin\alpha - \frac{U_B\cos\beta}{B}\right)\cos\delta \end{aligned} \tag{8}$$

where δ is power angle of the generator and Δ is:

$$\Delta = 1 - \frac{A}{B}\left(X_{ds}^{'} + X_{qs}\right) sin\left(\alpha - \beta\right) + \frac{A^2}{B^2} X_{qs} X_{ds}^{'} \quad (9)$$

III.2. Synchronous Machine

When line capacitance is neglected, the total series impedance of the line is R_e+jX_e. By neglecting R_e, the d and q components of the machine voltage, can be written as:

$$\begin{cases} u_d = \dfrac{X_q U_B \sin\delta}{X_{qe}} \\ u_q = \dfrac{X_d^{'} U_B \cos\delta}{X_{de}^{'}} + \dfrac{X_T + X_e}{X_{de}^{'}} E_q^{'} \end{cases} \quad (10)$$

where $X_{qe}=X_q+X_T+X_e$ and $X'_{de}=X'_d+X_T+X_e$. The emf in the quadrature axis is [27]:

$$E_q = \frac{X_{de}}{X_{de}^{'}} E_q^{'} - \frac{X_d - X_d^{'}}{X_{de}^{'}} U_B \cos\delta \quad (11)$$

where $X_{de}=X_d+X_T+X_e$. The dynamic of generator is represented by the third order model consisting of the electromechanical swing equation and the generator internal voltage equation [28]:

$$\begin{cases} \dfrac{d}{dt}\delta = \omega_o\left(\omega - 1\right) \\ \dfrac{d}{dt}\omega = \dfrac{1}{2H}\left(P_M - P_E - K_D\,\omega\right) \\ \dfrac{d}{dt}E_q^{'} = \dfrac{1}{T_{do}^{'}}\left[E_F - E_q^{'} + \left(X_d^{'} - X_d\right) i_d\right] \end{cases} \quad (12)$$

where E_F represents the voltage output voltage proportional to the internal voltage generator, ω is the rotor speed of the generator, P_M is the mechanical input power, K_D is the damping constant, J_M is the inertia constant and T'_{do} is direct axis transient open circuit time constant.

The damping of a system can be improved by controlling the output electrical power (P_E) of generator that depends on both angle δ and reactance of TCSC. The real power output of the generator is described as:

$$P_E = \frac{E_q^{'} U_B}{X_{de}^{'}} \sin\delta - \frac{U_B^2\left(X_q - X_d^{'}\right)}{2\,X_{qe} X_{de}^{'}} \sin 2\delta \quad (13)$$

The variation of output electrical power of the generator against the angle and TCSC reactance is shown in Fig. 6. Therefore, for a given δ, the value of P_E can be controlled by adjusting X_T.

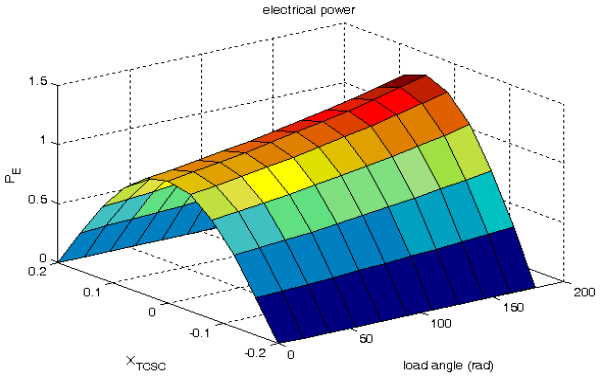

Fig. 6. Effect of rotor angle and TCSC reactance on output power of the generator

III.3. Exciter System

In most modern systems the AVR is a controller that senses the generator output voltage then initiates corrective action by changing the exciter control in the desired direction. There is a variety of different excitation types. The IEEE type-ST3 excitation is considered in this paper (Fig. 7).

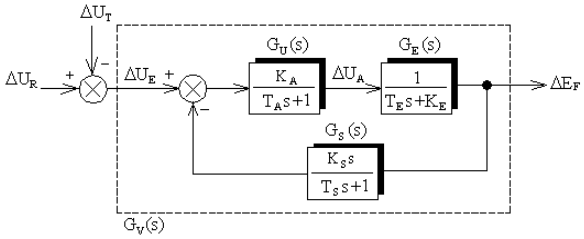

Fig. 7. IEEE type-ST3 excitation system

Error voltage signal U_E from voltage reference compared with terminal voltage is achieved. Block voltage regulator system, $G_U(s)$, with time constant T_A and K_A is interest. Shows the block transfer function $G_E(s)$, with two constant irritations to K_E and T_E. To increase the relative stability of the system maker stimulate sustainable used. $G_S(s)$ shows the block system stabilizers when stimulated with time constant T_S and gain K_S. The transfer function of the exciter is given by:

$$G_V\left(s\right) = \frac{\Delta E_F\left(s\right)}{\Delta U_E\left(s\right)} = \frac{G_U\left(s\right) G_E\left(s\right)}{1 + G_S\left(s\right) G_U\left(s\right) G_E\left(s\right)} \quad (14)$$

The exciter state space linearized equations can be written as:

$$\begin{cases} \dfrac{d}{dt}\Delta E_F = -\dfrac{K_E}{T_E}\Delta E_F + \dfrac{1}{T_E}\Delta U_A \\ \dfrac{d}{dt}\Delta U_A = \dfrac{K_A}{T_A}\Delta U_E - \dfrac{1}{T_A}\Delta U_A - \dfrac{K_A}{T_A}\Delta U_F \\ \dfrac{d}{dt}\Delta U_F = -\dfrac{K_S K_E}{T_S T_E}\Delta E_F + \dfrac{K_S}{T_S T_E}\Delta U_A - \dfrac{1}{T_S}\Delta U_F \end{cases} \quad (15)$$

III.4. TCSC Model

TCSC is one of the important members of FACTS family that is increasingly applied with long transmission lines by the utilities in modern power systems [29]. The control parameter of TCSC is its series reactance. The reactance of the line can be changed by TCSC. The block diagram of the TCSC with power oscillation damping (POD) controller is shown in Fig. 8, where K_T and T_T represent the gain and time constant of the TCSC. The input signal of the proposed controller is the speed deviation and output signal is the reactance offered by the TCSC.

The POD controller is consists of a gain block with gain K_C, a signal washout block with time constant T_C and two-stage lead-lag block with constants T_{C1}, T_{C2}, T_{C3} and T_{C4}.

It can achieve the desired damping ratio of the electromechanical mode and compensate for the phase shift between the control signal and the resulting electrical power deviation [30].

The TCSC can be described by the following dynamic equation:

$$\frac{d}{dt}X_T = -\frac{1}{T_T}X_T - \frac{K_T}{T_T}\left(U_S - X_{TR}\right) \tag{16}$$

where X_{TR} is the reference reactance.

IV. Linearized Incremental Model

Power sensitivity model is a linear analysis tool for the electric power systems. In the design of electromechanical mode damping controllers, the linearized incremental model around a nominal operating point is usually employed.

The d and q components of the machine current can be written as:

$$\begin{cases} \Delta i_d = K_{dd}\Delta\delta + K_{dt}\Delta X_T + K_{de}\Delta E_q^{'} \\ \Delta i_q = K_{qd}\Delta\delta + K_{qt}\Delta X_T + K_{qe}\Delta E_q^{'} \end{cases} \tag{17}$$

where the K constants are given by the following equations:

$$\begin{cases} K_{dd} = \dfrac{\begin{pmatrix} X_{qeo}U_B \sin\delta_o + \\ -R_e U_B \cos\delta_o \end{pmatrix}}{R_e^2 + X_{qeo}X_{deo}^{'}} \\ K_{dt} = \dfrac{R_e i_{qo} - X_{qeo} i_{do}}{R_e^2 + X_{qeo}X_{deo}^{'}} \\ K_{de} = \dfrac{X_{qeo}}{R_e^2 + X_{qeo}X_{deo}^{'}} \end{cases} \tag{18}$$

$$\begin{cases} K_{qd} = \dfrac{X_{deo}^{'}U_B \cos\delta_o + R_e U_B \sin\delta_o}{R_e^2 + X_{qeo}X_{deo}^{'}} \\ K_{qt} = \dfrac{X_{deo}^{'} i_{qo} - R_e i_{do}}{R_e^2 + X_{qeo}X_{deo}^{'}} \\ K_{qe} = \dfrac{R_e}{R_e^2 + X_{qeo}X_{deo}^{'}} \end{cases} \tag{19}$$

where the subscript "o" denotes the initial operation point.

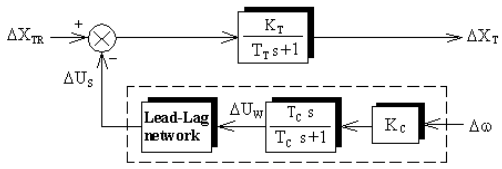

Fig. 8. Structure of the TCSC with lead-lag controller

The changes in the active electrical power delivered by the generator, the emf the quadrature axis and the generator terminal voltage are:

$$\Delta P_E = K_1\Delta\delta + K_P\Delta X_T + K_2\Delta E_q^{'} \tag{20}$$

$$\Delta E_q = \frac{1}{K_3}\Delta E_q^{'} + K_4\Delta\delta + K_Q\Delta X_T \tag{21}$$

$$\Delta U_T = K_5\Delta\delta + K_V\Delta X_T + K_6\Delta E_q^{'} \tag{22}$$

The constants K_1, K_2 and K_P, K_3, K_4 and K_Q and K_5, K_6 and K_V, shown above are given as follows:

$$\begin{cases} K_1 = \left(X_q - X_d^{'}\right)\left(I_{do}K_{qd} + I_{qo}K_{dd}\right) + K_{qd}E_{qo}^{'} \\ K_2 = K_{qe}E_{qo}^{'} + \left(X_q - X_d^{'}\right)\left(I_{do}K_{qe} + I_{qo}K_{de}\right) + I_{qo} \\ K_P = K_{qt}E_{qo}^{'} + \left(X_q - X_d^{'}\right)\left(I_{do}K_{qt} + I_{qo}K_{dt}\right) \end{cases} \tag{23}$$

$$\begin{cases} K_3 = \dfrac{1}{1 - \left(X_d^{'} - X_d\right)K_{de}} \\ K_4 = K_{dd}\left(X_d - X_d^{'}\right) \\ K_Q = K_{dt}\left(X_d - X_d^{'}\right) \end{cases} \tag{24}$$

$$\begin{cases} K_5 = \dfrac{U_{do}}{U_{TO}}X_q K_{qd} - \dfrac{U_{qo}}{U_{TO}}X_d^{'}K_{dd} \\ K_6 = \dfrac{U_{do}}{U_{TO}}X_q K_{qe} + \dfrac{U_{qo}}{U_{TO}} - \dfrac{U_{qo}}{U_{TO}}X_d^{'}K_{de} \\ K_V = \dfrac{U_{do}}{U_{TO}}X_q K_{qt} - \dfrac{U_{qo}}{U_{TO}}X_d^{'}K_{dt} \end{cases} \tag{25}$$

Fig. 9 block diagram representation of SMIB with TCSC. It can see that the damping torque contributions by the TCSC are the direct damping torque and the indirect damping torque.

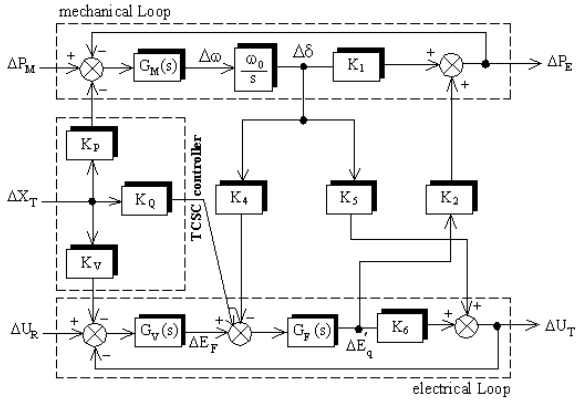

Fig. 9. Block diagram of the linearized SMIB model installed with TCSC

The state variable equations of the power system equipped with the TCSC can be represented as:

$$\frac{d}{dt}\Delta\omega = -\frac{K_D}{J_M}\Delta\omega - \frac{K_1}{J_M}\Delta\delta - \frac{K_2}{J_M}\Delta E_q^{'} + -\frac{K_P}{J_M}\Delta X_T + \frac{1}{J_M}\Delta P_M \quad (26)$$

$$\frac{d}{dt}\Delta\delta = \omega_o\Delta\omega \quad (27)$$

$$\frac{d}{dt}\Delta E_q^{'} = -\frac{K_4}{T_{do}^{'}}\Delta\delta - \frac{1}{K_3 T_{do}^{'}}\Delta E_q^{'} + + \frac{1}{T_{do}^{'}}\Delta E_F - \frac{K_Q}{T_{do}^{'}}\Delta X_T \quad (28)$$

$$\frac{d}{dt}\Delta E_F = -\frac{K_E}{T_E}\Delta E_F + \frac{1}{T_E}\Delta U_A - \frac{K_E K_V}{T_E}\Delta X_T \quad (29)$$

$$\frac{d}{dt}\Delta U_A = -\frac{K_5 K_A}{T_A}\Delta\delta - \frac{K_6 K_A}{T_A}\Delta E_q^{'} - \frac{1}{T_A}\Delta U_A + -\frac{K_A}{T_A}\Delta U_F + \frac{K_A K_V}{T_A}\Delta X_T + \frac{K_A}{T_A}\Delta U_R \quad (30)$$

$$\frac{d}{dt}\Delta U_F = -\frac{K_S K_E}{T_S T_E}\Delta E_F + \frac{K_S}{T_S T_E}\Delta U_A - \frac{1}{T_S}\Delta U_F \quad (31)$$

V. Simulation Results

Power systems are in general nonlinear systems and the operating conditions can vary over a wide range. The small signal stability analysis of an electrical power system is examined by the eigenvalues of the state matrix. To assess the effectiveness of the proposed controllers, four different loading conditions nominal, light, heavy, and leading power factor are considered for eigenvalue analysis. The data of the system are given in Table I [31].

TABLE I
SYSTEM DATA

Components	Value
Generator	X_d=0.973, X'_d=0.19, X_q=0.55, f=60 J_M=9.26, K_D=0, T'_{do}=7.76
Transmission line	R_e=0.034, X_e=0.997
Shunt load	G=0.249, B=0.262
Exciter (IEEE ST1-type)	T_A=0.05, K_A=50
Exciter (IEEE ST3-type)	T_A=0.05, K_A=50, T_E=0.5, K_E=-0.05 T_S=0.05, K_S=0.5
TCSC model	K_T=1, T_T=0.05, X_C=0.21, X_L=0.0525 X_{TO}=0.425, α_o=156^o
POD Controller	K_C=100, T_C=10, T_{C1}=0.07, T_{C2}=0.1 T_{C3}=0.08, T_{C4}=0.1
Normal loading	P_{EO}=1, Q_{EO}=0.015, U_{TO}=1.05
Light loading	P_{EO}=0.3, Q_{EO}=0.015, U_{TO}=1.05
Heavy loading	P_{EO}=1.1, Q_{EO}=0.1, U_{TO}=1.05
Leading power factor loading	P_{EO}=0.7, Q_{EO}=-0.3, U_{TO}=1.05

Fig. 10 present Bode diagram of the transfer function [$G_V(s)$] for various excitation system. It can be observed that the frequency bandwidth of IEEE type-ST1 is higher than the IEEE type-ST3. The speed of response is increased with an increase in the bandwidth.

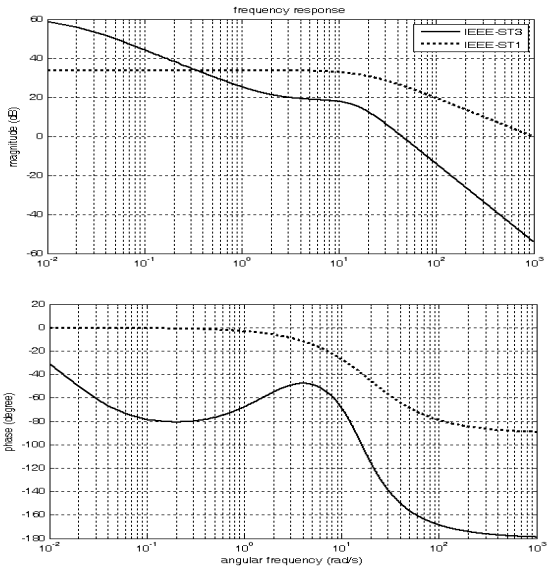

Fig. 10. Bode plot of voltage error to output excitation system IEEE type-ST3 (solid) and IEEE type-ST1 (dotted)

The value of the sensitivity constant of model power system with the proposed controller for different of loading conditions are given in Table II.

The system eigenvalues with and without the controller for normal loading, light loading, leading power factor loading and heavy loading conditions are given in Tables III, IV, V and Table VI, which shows the electrometrical mode eigenvalue with its damping ratio. This base syste-

m has a negatively-damped electromechanical mode and needs to be stabilized by supplementary TCSC control. Therefore, with addition of the TCSC, the system has become very stable.

TABLE II
CONSTANT PARAMETERS

Constant	Normal	Light	Leading power factor	Heavy
K_P	-0.6539	-0.1717	-0.3858	-0.7458
K_V	-0.0669	-0.0060	-0.0875	-0.0626
K_Q	-0.2292	-0.0278	0.0136	-0.3022
K_{dd}	0.7343	0.0758	0.5931	0.7777
K_{dt}	-0.2927	-0.0355	0.0173	-0.3859
K_{de}	0.6980	0.6980	0.6980	0.6980
K_{qd}	0.1375	0.3805	0.4462	0.0442
K_{qt}	-0.4783	-0.1572	-0.4044	-0.5008
K_{qe}	0.0132	0.0132	0.0132	0.0132

TABLE III
SYSTEM EIGENVALUES OF NOMINAL LOADING CONDITION

Case	IEEE type-ST1	IEEE type-ST3
Without TCSC	0.2659±j 4.9547 (-0.054) -10.3642±j3.3940	-0.0064±j4.6228 (0.001) -0.4940±j1.5008 -10.5473±j10.4017
With TCSC	-3.8253±j2.9073 (0.796) -11.5759±j1.0693 -5.4377±j6.3810 -18.5184 -0.1032	-0.4114±j1.7014 (0.235) -4.0960±j7.4737 -5.6346±j6.1060 -18.1672 -11.3756 -2.1360 -0.1031

TABLE IV
SYSTEM EIGENVALUES OF LIGHT LOADING CONDITION

Case	IEEE type-ST1	IEEE type-ST3
Without TCSC	-0.0228±j 4.8540 (0.005) -10.0755±j3.8380	-0.0147±j4.8804 (0.003) -0.5003±j1.3367 -10.5333±j10.3615
With TCSC	-0.9375±j4.3567 (0.210) -10.0172±j3.5144 -19.4879 -10.8628 -7.9380 -0.1011	-0.9373±j4.4114 (0.208) -0.7142±j1.4557 -5.2500±j6.4088 -19.4796 -10.9012 -7.7809 -0.1011

TABLE V
SYSTEM EIGENVALUES OF LEADING LOADING CONDITION

Case	IEEE type-ST1	IEEE type-ST3
Without TCSC	0.0004±j 5.4821 (0.000) -10.0988±j3.2894	-0.0537±j5.4811 (0.010) -0.4457±j1.3516 -10.5489±j10.3825
With TCSC	-2.0769±j4.9491 (0.387) -6.8567±j4.5954 -11.5593±j1.1093 -19.2122 -0.1013	-2.4675±j6.1686 (0.371) -0.5601±j1.5122 -5.3147±j6.1232 -18.8840 -11.1662 -5.2300 -0.1013

TABLE VI
SYSTEM EIGENVALUES OF HEAVY LOADING CONDITION

Case	IEEE type-ST1	IEEE type-ST3
Without TCSC	0.3827±j4.7243 (-0.081) -10.4811±j3.4599	0.0424±j4.1836 (-0.010) -0.5446±j1.6044 -10.5462±j10.4093
With TCSC	-3.6910±j2.0775 (0.871) -5.6520±j7.0900 -11.6022±j1.0680 -18.3048 -0.1041	-0.2960±j1.7406 (0.168) -5.6969±j6.2108 -4.4776±j7.8929 -17.9331 -11.4327 -1.6552 -0.1039

For the design purpose, the model of example power system which is a SMIB power system installed with the proposed controllers is developed in Matlab Simulink as shown in Fig. 11.

Simulation results the power angle deviation and rotor speed deviation for step change in input mechanical power at normal loading condition are shown in Figs. 12 and 13.

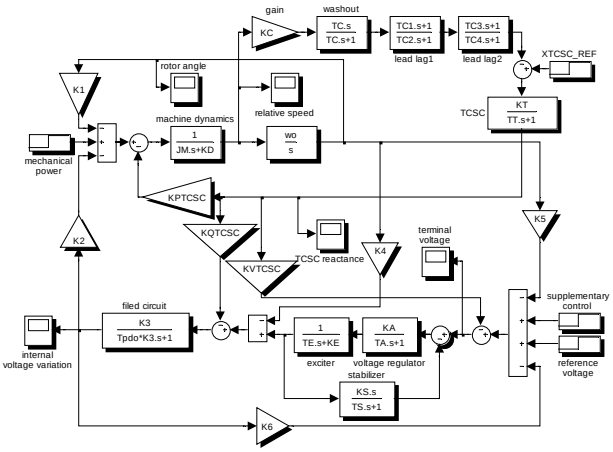

Fig. 11. Bode plot of voltage error to output excitation system

The control effort provided by the reactance of TCSC at normal loading condition for different excitation system is shown in Fig. 14. It can be readily seen that the IEEE type-ST1 performance better than IEEE type-ST3 in terms of reduction of overshoot and setting time.

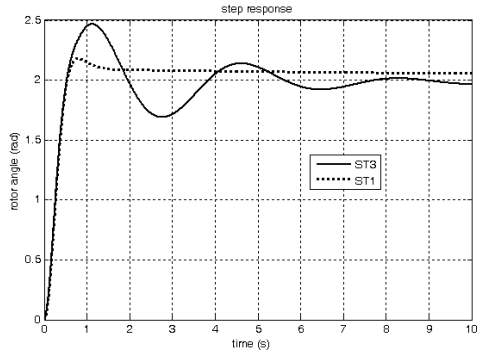

Fig. 12. Step response of rotor angle at normal loading condition

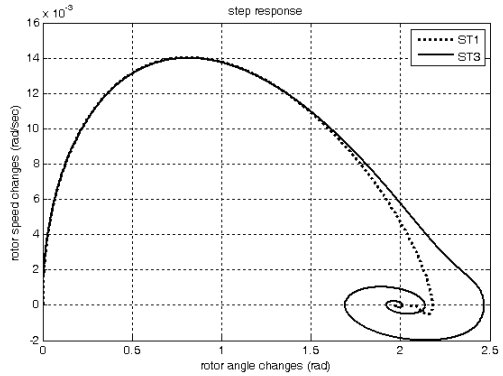

Fig. 13. System trajectory at normal loading condition

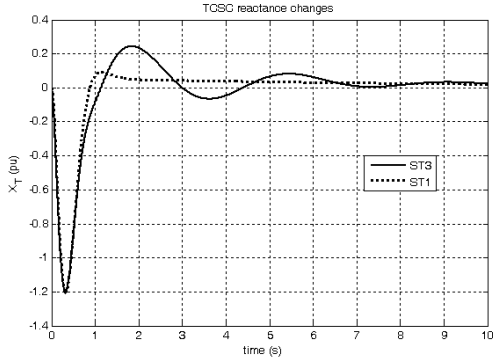

Fig. 14. Step response of rotor speed at normal loading condition

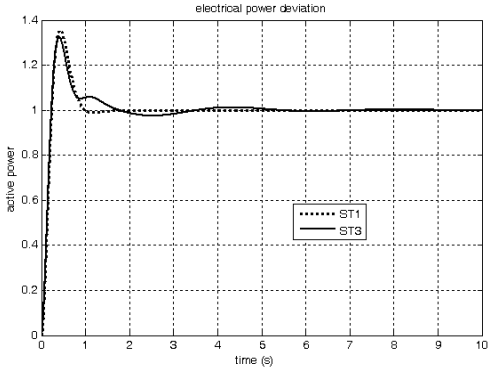

Fig. 15. Step response of electrical power at normal loading condition

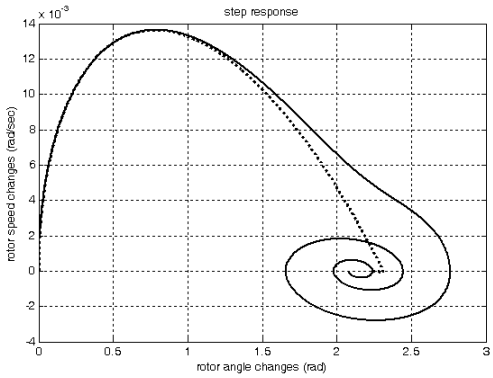

Fig. 16. System trajectory at light loading condition

Fig. 15 show the comparison of active power deviation for the cases with IEEE type-ST1 and IEEE-type-ST3. The power angle deviation and rotor speed deviation for step change in input mechanical power at heavy loading condition is shows in Fig. 16. Simulation results show that TCSC with POD controller can indeed improve the damping of the power systems.

VI. Conclusion

TCSC is a power electronic-based device that provides a fast and controllable series compensation of transmission line reactance. By modifying the line reactance TCSC acts as either inductive or capacitive compensator.

In this paper, improvement of power system damping through control of TCSC has been investigated in SMIB power system by power sensitivity model. For the proposed POD controller, an eigenvalue-based objective function to increase the damping of the system oscillation was developed. The simulation results of the power system with two excitation system indicate robust performance with load changes. Based on the time domain results, it is obvious that IEEE type-ST1 is a better option as it damp out oscillation faster than IEEE type-ST3.

Acknowledgements

This work has been extracted from the research project entitled “Analysis and simulation of the effect thyristor controlled FACTS devices for power system damping enhancement” in Najafabad Branch, Islamic Azad University, Esfahan, Iran.

References

[1] T.T. Ma, "Space vector model and control of a two-leg four-switch STATCOM", *International Review of Electrical Engineering (IREE)*, Vol.5. No.3, June 2010.

[2] M.A. Furini, P.B. de Araujo, "A comparative study of the damping oscillation function of TCSC and UPFC", *IEEE/PES*, pp.1-6, Aug. 2008.

[3] D. Rai, G. Ramakrishan, S.O. Faried, A.A. Edris, "Enhancement of power system dynamics using a phase imbalanced series compensation scheme", *IEEE Trans. on Pow. Sys.*, Vol.25, No.2, pp.966-974, May 2010.

[4] J.V. Milanovic, Y. Zhang, "Global minimization of financial losses due to voltage sags with FACTS based devices", *IEEE Trans. on Pow. Deli.*, Vol.25, No.1, pp.298-306, Jan. 2010.

[5] G. Shahgholian, J. Faiz, "Static synchronous compensator for improving performance of power system: A review", *International Review of Electrical Engineering (IREE)*, Vol.4, No.2, pp., Oct. 2010.

[6] D. Jovcic, N. Pahalawaththa, M. Zavahir, H.A. Hassan, "SVC dynamic analytical model ", *IEEE Tran. on Pow. Deli*, Vol.18, No.4, pp.1455-1461, Oct. 2003.

[7] M.R.S. Tirtashi, K. Mazlumi, M. Sadeghi, "TCPS controller design using PSO and chaos algorithm to damping the power system oscillations", *IEEE/ECTI-CON*, pp.1191-1195, Chaing Mai, May 2010.

[8] A.M. Parimi, I. Elamvazuthi, N. Saad, "Improvement of power system stability with fuzzy logic based IPFC", *International Review of Electrical Engineering (IREE)*, Vol.5. No.3, June 2010.

[9] K. Sedraoui, F. Fnaiech, K. Al-Haddad, "Solutions for power quality using the advanced UPFC – control strategy and case study", *International Review of Electrical Engineering (IREE)*, Vol.3, pp.811-819, 2008.
[10] S.J. Gole, A.M. Annakkage, U.D. Jacobson, "Damping performance analysis of IPFC and UPFC controllers using validated small-signal models", *IEEE Trans. on Pow. Deli*., Vol.26, No.1, pp.446-460, Jan. 2011.
[11] M.O. Hassan, Z.A. Zakaria, S.J. Cheng, "Impact of TCSC on Enhancing Power System Stability", *IEEE/APPEEC*, pp.1-6, Mar. 2009.
[12] L. A.S. Pilotto,A. Bianco, W.F. Long, A. Edris,"Impact of TCSC control methodologies on subsynchronous oscillations", *IEEE Trans. on Pow. Del*., Vol.18, No.1, pp.242-252, Jan. 2003.
[13] N. Magaji, M.W. Mustafa, "Optimal location of TCSC device for damping oscillations", *ARPN Jour. of Eng. and Appl. Scie*., Vol.4, No.3, May 2009.
[14] Y.C. Chang, R.F. Chang, T.Y. Hsiao, C.N. Lu, "Transmission system loadability enhancement study by ordinal optimization method*", IEEE Trans. on Pow. Sys*., Vol.26, No.1, pp.451-459, Feb. 2011.
[15] S.R. Wagh, A.K. Kamath, N.M. Singh, "Non-linear model predictive control for improving transient stability of power system using TCSC controller", *IEEE/ASCC*, pp.1627-1632, Aug. 2009.
[16] L.D. Colvara, S.C.B. Araujo, E.B.Festraits, "Stability analysis of power system including facts (TCSC) effects by direct method appraoch", *Elec. Pow. and Ene. Sys*., pp.264-274, No.27, 2005.
[17] X. Li, L. Bao, X. Duan, Y. He, M. Gao, "Effects of FACTS controllers on small-signal voltage stability", *IEEE/PESW*, Vol.4, pp.2793-2799, Jan. 2000.
[18] A. Deihimi, H. Javaheri, "A Fuzzy multi-objective multi-case genetic-based optimization for allocation of FACTS devices to improve system static security, power loss and transmission line voltage profiles", *International Review of Electrical Engineering (IREE)*, Vol.5, No.4, Aug. 2010.
[19] N. Magaji, M.W. Mustafa, "Determination of best location of FACTS devices for damping oscillations", *International Review of Electrical Engineering (IREE)*, Vol.5. No.3, June 2010.
[20] M. Hadef, M.R. Mekideche, H.Allag, "Relative magnetic permeability identification of the permanent magnets of a synchronous motor using inverse problem", *International Review of Electrical Engineering (IREE)*, Vol.2, No.2, pp.103-109, Feb. 2007.
[21] S. Biansoongnern, S. Chusanapiputt, S. Phoomvuthisarn, "Optimal SVC and TCSC placement for minimization of transmission losses", *IEEE/ICPST*, 2006.
[22] L. Fan, A. Feliachi, K. Schoder, "Selection and design of a TCSC control sugnal in damping power system inter-area oscillations for multiple operating conditions", *Elec. Pow. Sys. Res*., Vol.62, pp.127-137, 2002.
[23] S. Panda, N.P. Padhy, "Power system with PSS and FACTS controller: Modeling, simulation and simultaneous tuning employing genetic algorithm", *Inte. Jou. Elec. Com. Sys. Eng*., Vol.1, No.1, pp.9-18, winter 2007.
[24] S. Panda, N.P.Padhy, "Thyristor controlled series compensator based controller design employing genetic algorithm: A comparative study", *Int. Jou. of Elec., Cir. and Sys*., Vol.1, No.1, pp.38-47, 2007.
[25] H.Li, Q.H.Wu, D.R.Turner, P.Y.Wang, X.X.Zhou, "Modeling of TCSC dynamics for control and analysis of power system stability", *Elec. Pow. And Ener. Sys*., Vol.22, pp.43-49, 2000.
[26] A. Luo, Z. Shuai, W. Zhu, Z. J. Shen, "Combined system for harmonic suppression and ractive power compensation", *IEEE Tran. on Ind. Ele*., Vol.56, No.2, pp.418-428, Feb. 2009.
[27] L. Cong, Y. Wang, D.J. Hill, "Transient stability and voltage regulation enhancement via coordinated control of generator excitation and SVC", *Elec. Pow. and Eng. Sys*., pp.121-130, 2005.
[28] G. Shahgholian, "Development of state space model and control of the STATCOM for improvement of damping in a single-machine infinite-bus", *International Review of Electrical Engineering (IREE)*, Vol.4, No.6, pp.1367-1375, Nov./Dec. 2009.
[29] S. Panda, S. C. Swain, A. K. Baliarsingh, A. K. Mohanty, C. Ardil, "Multi-objective optimization with fuzzy based ranking for TCSC supplementary controller to improve rotor angle and voltage stability", *Int. Jour. of Elec. Pow. and Ene. Sys. Eng*., pp.25-32, 2009.
[30] A.S.P. Kanojia, B.V.K. Chandrakar, "Damping of power system oscillations by using coordinated tuning of POD and PSS with STATCOM", *Worl. Acad. of Sci., Eng. and Tec*., pp.1066-1071, Vol.50, 2009
[31] S.M. Bamasak, "*FACTS based stabilizers for power system stability enhancement*", Ms. Thesis, Dhahran, Saudi Arabia, May 2005.

Authors' information

Department of Electrical Engineering,
Najafabad Branch, Islamic Azad University,
Najafabad, Esfahan, Iran.

Ghazanfar Shahgholian was born in Esfahan, Iran, on Dec. 7, 1968. He graduated in electrical engineering from Isfahan University of Technology (IUT), Esfahan, Iran, in 1992. He received the M.Sc and PhD in electrical engineering from University Tabriz, Tabriz, Iran in 1994 and Science and Research Branch, Islamic Azad University, Tehran, Iran, in 2006, respectively. He is now an associate professor at Department of Electrical Engineering, Faculty of Engineering, Islamic Azad University Najafabad Branch. He is the author of 100 publications in international journals and conference proceedings. His teaching and research interests include application of control theory to power system dynamics, power electronics and power system simulation.

Afshin Etesami was born in Esfahan, Iran, on January 27, 1978. He graduated in electrical engineering from Najafabad Branch, Islamic Azad University, in 2001. He received the M.Sc in electronic engineering from Najafabad Branch, Islamic Azad University, in 2004. His teaching and research interests include power system dynamics, electrical machine and power system simulation.